

Hemodynamic and Histologic Characterization of a Swine (*Sus scrofa domestica*) Model of Chronic Pulmonary Arterial Hypertension

Abraham Rothman,^{1,2,*} Robert G Wiencek,³ Stephanie Davidson,⁴ William N Evans,^{1,2} Humberto Restrepo,^{1,2} Valeri Sarukhanov,¹ Amanda Rivera-Begeman,⁵ and David Mann⁶

The purpose of this work was to develop and characterize an aortopulmonary shunt model of chronic pulmonary hypertension in swine and provide sequential hemodynamic, angiographic, and histologic data by using an experimental endoarterial biopsy catheter. Nine Yucatan female microswine (*Sus scrofa domestica*) underwent surgical anastomosis of the left pulmonary artery to the descending aorta. Sequential hemodynamic, angiographic, and pulmonary vascular samples were obtained. Six pigs (mean weight, 22.4 ± 5.3 kg; mean age, 7.3 ± 2.7 mo at surgery) survived long-term (6 mo) and consistently developed marked pulmonary arterial hypertension. Angiography showed characteristic central pulmonary arterial enlargement and peripheral tortuosity and pruning. The biopsy catheter was safe and effective in obtaining pulmonary endoarterial samples for histologic studies, which showed neointimal and medial changes. Autopsy confirmed severe pulmonary vascular changes, including concentric obstructive neointimal and plexiform-like lesions. This swine model showed hemodynamic, angiographic, and histologic characteristics of chronic pulmonary arterial hypertension that mimicked the arterial pulmonary hypertension of systemic-to-pulmonary arterial shunts in humans. Experimental data obtained using this and other models and application of an in vivo endoarterial biopsy technique may aid in understanding mechanisms and developing therapies for experimental and human pulmonary arterial hypertension.

Abbreviations: LPA, left pulmonary artery; PAH, pulmonary arterial hypertension.

Despite the advent of new therapeutic agents in the past decade, pulmonary arterial hypertension (PAH) continues to be a serious disease, with a poor prognosis and a complex and incompletely understood pathophysiology. PAH is defined as a mean pulmonary artery pressure greater than 25 mm Hg with a normal pulmonary artery wedge pressure (≤ 15 mm Hg) and an increased pulmonary vascular resistance (PVR; ≥ 3 Wood units/ m^2).³⁹ Histologic pulmonary vascular changes in PAH include medial hypertrophy, intimal lesions, and adventitial thickening. Experimental models of PAH have been developed in rats, mice, dogs, sheep, pigs, cows, and nonhuman primates.^{3,5,6,10,12,15,19,22,23,26,27,29,32,44,48,53} Small animal models offer the advantage of the availability of numerous subjects and easier experimental manipulation. Large animal models allow in vivo evaluation through cardiac catheterization and endovascular biopsy of pathophysiology that is similar in scale to humans. The most common methods for creating PAH have included hypoxia, monocrotaline infusion, embolic occlusion, and creation of aortopulmonary shunts.^{3,5,6,10,12,15,19,20,22,23,26,27,29,32,44,48,53} One model⁷ involves the creation of chronic PAH in swine by anastomosis of the left pulmonary artery (LPA) to the descending aorta. We further modified this model and provide sequential hemodynamic, angiographic, and

histologic data by using an experimental endoarterial biopsy catheter.

Materials and Methods

The investigation conformed to the *Guide for the Care and Use of Laboratory Animals*.¹⁸ The University of Nevada of Las Vegas Institutional Animal Subjects Committee approved the study protocol. Yucatan female microswine ($n = 9$; mean weight, 22.4 ± 5.3 kg; mean age, 7.3 ± 2.7 mo; Sinclair Research Center, Columbia, MO) were used for creating the aortopulmonary shunt model of chronic PAH.

Baseline right-sided cardiac catheterization with pulmonary angiography and biopsy was performed with a 7-French wedge catheter, advanced through an 8-French sheath in a right internal jugular vein. Induction of anesthesia consisted of a mixture of ketamine hydrochloride (22 mg/kg IM; Ben Venue Laboratories, Bedford, OH), acepromazine (0.2 mg/kg IMs; Vedco, St Joseph, MO), and atropine (0.05 mg/kg IM; Baxter Healthcare, Deerfield, IL). Anesthesia was maintained with inhaled isoflurane (Baxter Healthcare) 0.5 to 2.0%. The pigs were ventilated at a rate of 12 to 18 breaths per minute. Cefazolin (1 g IV; West-Ward Pharmaceutical, Eatontown, NJ) was administered before the procedure and 12 h later. To prevent ventricular arrhythmias, amiodarone (10 to 12 mg/kg IV; Bioniche Pharma, Lake Forest, IL) was administered prior to catheterization.

The biopsy catheter and procedure have been described previously.^{40,42} Briefly, the short 8-French sheath was exchanged for an 8-French long Mullins sheath, which was wedged in a 2- to 3-mm

Received: 15 Nov 2010. Revision requested: 08 Dec 2010. Accepted: 18 Dec 2010.

¹Children's Heart Center-Nevada, ²Division of Cardiology, Department of Pediatrics, University of Nevada School of Medicine, ³Cardiovascular Surgical Associates, ⁴Anesthesiologist Consultants, and ⁵Laboratory Medicine Consultants, Las Vegas, Nevada; ⁶Vascular BioSciences, Durham, North Carolina.

*Corresponding author. Email: rothman@childrensheartcenter.com

peripheral pulmonary artery. An angiogram was performed in the vessel by instilling 3 to 5 mL of contrast manually. Several biopsy samples were obtained in each vessel.

For surgical creation of the aortopulmonary anastomosis, a left thoracotomy was performed in the fourth intercostal space. The LPA was exposed, clamped, divided, and ligated at its origin from the pulmonary trunk. Heparin was given (100 U/kg). The descending thoracic aorta was clamped, and a window was created in its medial aspect by using a punch (ClearCut, Quest Medical, Oconomowoc, WI). An end-to-side anastomosis was created. The vascular clamp in the aorta was released, and furosemide (2 mg/kg; IVX Animal Health, St Joseph, MO) was given. The chest was closed. No chest tube was placed in any of the pigs.

Postoperatively, pigs received furosemide orally (2 to 4 mg/kg twice daily for 3 to 4 wk; Vintage Pharmaceuticals, Huntsville, AL), cephalexin capsules (500 mg twice a day for 10 d; Teva Pharmaceuticals, North Wales, PA), and buprenorphine (Reckitt Benckiser Pharmaceutical, Parsippany, NJ) 0.01 to 0.02 mg/kg twice daily for 5 d and then as needed if swine showed lack of activity, decreased consumption of food or water, or increased recumbency. No chronic anticoagulant or antiplatelet drugs were given.

Catheterization with aortic pressure and LPA pressure measurement, angiography, and biopsies of the LPA were performed at 1 and 3 wk and monthly from 2 to 6 mo after surgery. Vascular access was from a carotid artery, isolated by cutdown, and cannulated with an 8-French sheath. A cutoff 5-French pigtail catheter was used to enter the LPA from the proximal descending aorta by using a Wholey wire. Angiograms of proximal and distal LPA branches were performed before and after biopsy through the pigtail catheter or long sheath. At least 8 biopsy samples were obtained from each pig during catheterization. The hole in the carotid artery was repaired with nonabsorbable sutures.

Pigs were euthanized by using intravenous pentothal sodium (120 mg/kg). The heart and lungs were examined. Cross-sections of arteries and parenchyma were obtained for histologic examination.

Results

Yucatan microswine ($n = 9$) underwent surgical anastomosis of the LPA to the proximal descending aorta as previously described⁷ (Figure 1). Three pigs with connections ranging from 6 to 8 mm in diameter (size of surgical window in the aorta) died within 1 wk of the surgery with signs of massive pulmonary edema. The remaining 6 pigs, which had connections of 4.5 mm in diameter, survived 180 d after the surgery and developed systemic level PAH. Figure 2 shows the systolic LPA pressure (as a ratio of systemic pressure) compared with time after surgery in the 6 long-term survivors.

LPA angiography performed after surgery (while pressure was still normal) showed smooth and undistorted distal pulmonary artery branches. After the onset of severe PAH, the proximal branches became enlarged, with occasional evidence of filling defects consistent with thrombus, tortuosity, narrowing, irregularities, and a reduction in number of distal LPA branches (Figure 3). Angiograms obtained immediately after the biopsies generally showed patent and undistorted vessels; there were occasional partial narrowings or irregularities in the luminal contour, but rarely complete occlusions. At follow-up angiography, vascular changes, including total occlusions, usually had resolved. There were no other complications of the procedure, including death,

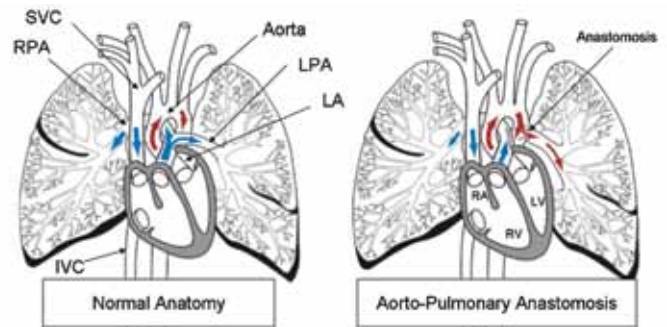


Figure 1. Schematic of normal anatomy and the aortopulmonary anastomosis. At surgery, the left pulmonary artery (LPA) was connected to the descending aorta. IVC, inferior vena cava; LA, left atrium; LV, left ventricle; RA, right atrium; RV, right ventricle; SVC, superior vena cava.

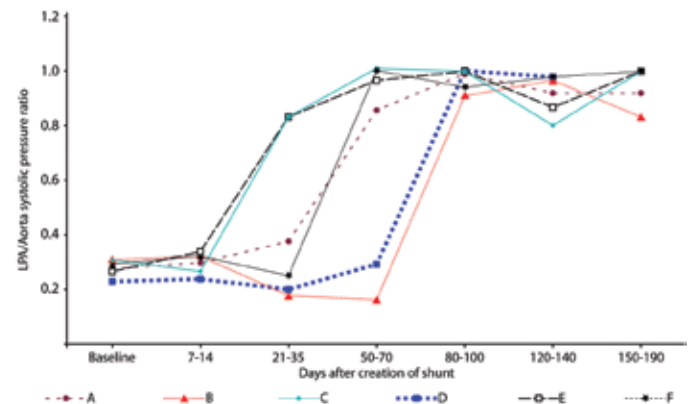


Figure 2. Left pulmonary artery (LPA) systolic pressure (as a ratio of systemic systolic pressure) compared with time after surgical shunt creation in 6 micropigs that survived long-term.

hypotension, arrhythmias, hemothorax, hemoptysis, and difficulties with weaning from anesthesia.

The size of the biopsy samples was sufficient for histologic examination, including hematoxylin and eosin, trichrome, and elastin stains. Baseline samples demonstrated normal architecture, with a thin layer of endothelium and uniform layers of elastin. Biopsy samples from the high-flow but low-pressure stage showed minimal thickening of the neointima, endothelial cell changes, and mild disorganization of elastic laminae. Biopsy samples from hypertensive vessels showed more severe endovascular changes, including progressive thickening of the neointima (Figure 4). Biopsy samples were also sufficient for molecular studies, including DNA microarray analysis and quantitation of microRNA expression at different stages of PAH (data not shown).

At necropsy, the hypertensive left lung was grossly congested with reddish-purple discoloration but without external signs of biopsy-related trauma. The pulmonary arterial wall was thickened, with variable amounts of intraluminal thrombus (2 pigs showed large thrombi, 1 with complete occlusion from the aortic anastomosis to the periphery), yellow discoloration, and irregular surfaces (Figure 5). Some vessels showed significant patchy sclerosis, which was impossible to cut with a sharp scalpel. The heart was normal. On histologic examination, the parenchyma of the hypertensive left lung showed changes consistent with severe pulmonary hypertension, including

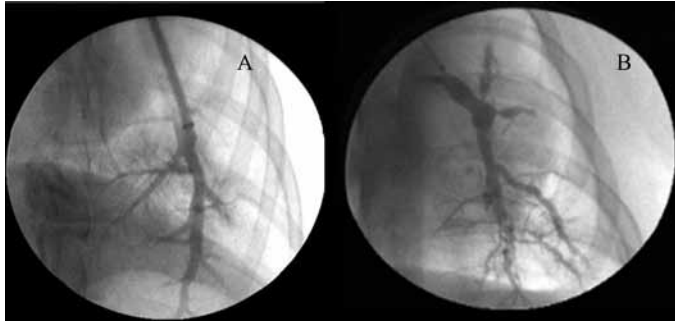


Figure 3. (A) Pulmonary arteriogram in a normal, nonhypertensive micropigs. (B) Left pulmonary artery angiograms after development of systemic level pulmonary arterial hypertension, showing proximal dilation, peripheral tortuosity, and marked pruning with loss of branching vessels.

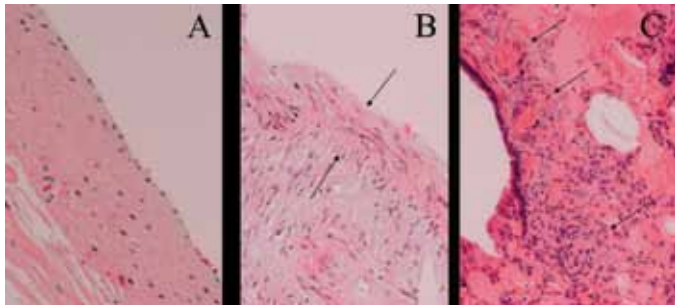


Figure 4. (A) Endoarterial biopsy samples obtained at baseline from presurgical, normal pulmonary artery. Hematoxylin and eosin stain; magnification, $\times 40$. (B) Postsurgical left pulmonary artery with systemic pulmonary hypertension, showing thickened neointima (arrows) and disorganized medial layer. Hematoxylin and eosin stain; magnification, $\times 40$. (C) Specimen of the left (hypertensive) lung at time of necropsy, showing vascular occlusive and plexiform-like lesions. Hematoxylin and eosin stain; magnification, $\times 10$.

thickening of the neointima, degenerative changes in the media, concentric occlusive neointimal lesions, and plexiform-like lesions (Figure 4).

Discussion

We describe the hemodynamic, angiographic, and histologic features of a swine aortopulmonary shunt model of chronic pulmonary hypertension by using sequential endoarterial biopsy. This model mimics systemic-to-pulmonary arterial shunts in humans including patent ductus arteriosus, Potts shunts (anastomosis of the left pulmonary artery to the descending aorta), Waterston shunts (anastomosis of the right pulmonary artery to the ascending aorta), large Blalock-Taussig shunts, hemitruncus (origin of one of the pulmonary arteries from the ascending aorta), aortopulmonary windows, and perhaps even ventricular septal defects.

The use of a 4.5-mm aortic window in Yucatan microswine established a reproducible hemodynamic course, which allowed for 1 or 2 catheterizations while the LPA pressure was still normal and several subsequent catheterizations and biopsy procedures when severe PAH had developed. This PAH model can now be used to test therapeutic agents or maneuvers at several hemodynamic and disease stages, including prior to shunt surgery,

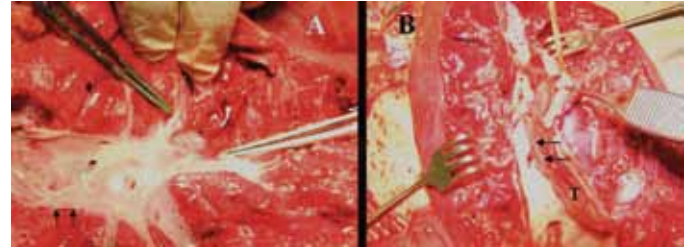


Figure 5. Specimens of (A) right and (B) left lungs obtained at the time of necropsy. (A) The right pulmonary artery (normotensive lung) shows a smooth wall (arrows) with normal thickness. (B) The left pulmonary artery (hypertensive lung) shows considerable thickening of the wall (arrows) and a thrombus (T) partially occluding the lumen.

during the high-flow but low-pressure state, and at the time of development of PAH.

Some procedural details were important in the final development of the model. Unique features were the size of the aortic window at the time of surgery and continuous use of furosemide twice daily for 3 to 4 wk. No chest tubes were used. Antibiotics were continued for 10 d after surgery and reinstated when pigs had increased coughing or fevers. Neither antiplatelet agents nor anticoagulants were used, except for heparin during the surgery and catheterization procedures. However, 2 pigs showed prominent thrombi in the LPA vascular tree at necropsy, 1 with complete occlusion from the aorto-LPA anastomosis to the periphery. Therefore, we recommend chronic use of antiplatelet or anticoagulant agents if pigs are maintained longer than 3 to 4 mo.

Another unique aspect of the current study was the use of an experimental endoarterial biopsy catheter, which allowed sequential pulmonary vascular biopsy procedures as the PAH model developed. The catheter was safe. Biopsy procedures were performed without complication as early as 6 d after the surgical anastomosis site was created. Vascular changes, including spasm, thrombosis, and vessel irregularities, were rare and did not cause significant hemodynamic effects. The vast majority of vascular changes resolved on follow-up angiography. The pigs recovered easily from the biopsy procedures and anesthesia; there were no deaths related to the biopsy procedure. In a previous model created by repeated delivery of microspheres to the pulmonary vasculature, sites of biopsies done immediately after the procedure showed small indentations or endovascular flaps.⁴⁰ However, examination of the luminal surface of arteries more than 6 mo after biopsy showed no indentations or vascular flaps and no evidence of extravascular blood or aneurysms.⁴⁰

The biopsy catheter was effective. Procurement of biopsy samples at normal pulmonary arterial pressures was easy and relatively simple. Despite partial occlusion by endovascular thickening and thrombus, biopsy samples in pulmonary arteries could still be obtained at systemic-level pressures. Previous studies⁴² have shown that these biopsy samples were adequate for cell culture and propagation of smooth muscle and endothelial cells and histology studies. The average biopsy sample cross-section measured on slides was 1.1 mm in length and 0.4 mm in depth. Clearly identifiable endothelium was present in the biopsy samples of 17 of the 25 procedures (68%).⁴² Samples from hypertensive dogs and swine showed progressive thickening of the neointima, mostly composed of connective tissue and a few smooth muscle cells, degenerative changes, and disorganized elastic laminae in the media. A previous study also found that biopsy samples obtained

in an experimental model of lung transplantation were adequate for PCR analysis and that molecular changes in mRNA levels of vascular cell adhesion molecule 1 preceded histologic changes of lung transplant rejection.⁴¹ Furthermore, biopsy samples from our current swine model have supported preliminary analysis of DNA, mRNA transcripts, and microRNAs (studies in progress). We have used the biopsy catheter safely and effectively in more than 1000 experimental pulmonary arterial biopsy attempts.

Although prostacyclin analogs, endothelin blockers, and phosphodiesterase 5 inhibitors have been approved for treatment of patients with PAH,^{13,14,17,24,31,37,38,46,51} it continues to be a progressive disease with significant morbidity and mortality. A helpful approach to better understand the mechanisms leading to PAH and to develop additional therapies may be to use animal models and devise techniques to obtain pulmonary vascular tissue in animals and humans. PAH has been created in small animal models, including mice and rats, by using hypoxia,^{5,10,23,48} monocrotaline,^{6,12,15,19,22,26,29,44,53} genetic modifications,^{1,19,47,52} and surgical shunts.²⁰ A limitation of these models is difficulty with chronic hemodynamic and tissue monitoring. Large animal models, including pigs, sheep, dogs, macaques, calves, and apes, have been created by using hypoxia,^{2,8,21,33,43,45,49,50} monocrotaline,^{4,16,30} infectious agents,²⁵ and surgery.^{3,7,9,11,27,28,32,34-36,40,42} These models have contributed to the understanding of PAH. Use of the endoarterial biopsy catheter, as described earlier, now adds the potential of sequential study of vascular tissue at different stages of PAH evolution and therapy.

Our current model has several limitations. Pigs may not exactly reflect the changes or rate of development of PAH that occur in humans. We did not perform direct assessment of LPA vascular resistance because the amount of flow through the left lung was not quantified. Fluoroscopy in the animal lab was not as optimal in quality as in clinical catheterization laboratories; therefore minor vascular changes during model progression or after biopsy procedures may have been characterized incompletely.

Research in the Yucatan micropig and other animal models can be expanded by the use of genetic information obtained from the biopsy samples to learn more about the pathophysiology and staging of PAH and to develop new gene-, mRNA-, or microRNA-based therapies. In addition, genetic and structural endovascular changes can be tracked with biopsies in the course of a specific therapy. Application of this biopsy catheter may increase our understanding and open new avenues for therapy in human PAH.

Acknowledgments

We thank Dr Ruben J Acherman for figure preparation, Debbie Nichols for histology slide preparation, Drs Ivan McMurtry and Namasivayam Ambalavanan for histologic advice, and the late Dr Kenneth Moser for his mentorship.

References

1. **Beppu H, Ichinose F, Kawai N, Jones RC, Yu PB, Zapol WM, Miyazono K, Li E, Bloch KD.** 2004. BMPRII heterozygous mice have mild pulmonary hypertension and an impaired pulmonary vascular remodeling response to prolonged hypoxia. *Am J Physiol Lung Cell Mol Physiol* **287**:L1241–L1247.
2. **Berkenbosch JW, Baribeau J, Perreault T.** 2000. Decreased synthesis and vasodilation to nitric oxide in piglets with hypoxia-induced pulmonary hypertension. *Am J Physiol Lung Cell Mol Physiol* **278**:L276–L283.
3. **Bousamra M 2nd, Rossi R, Jacobs E, Parviz M, Busch C, Nelin LD, Haworth S, Dawson CA.** 2000. Systemic lobar shunting induces advanced pulmonary vasculopathy. *J Thorac Cardiovasc Surg* **120**: 88–98.
4. **Chen EP, Bittner HB, Davis RD, Van Trigt P.** 1997. Right ventricular failure—insights provided by a new model of chronic pulmonary hypertension. *Transplantation* **63**:209–216.
5. **Chen SJ, Chen IF, Meng QC, Durand J, Dicarulo VS, Oparil S.** 1995. Endothelin-receptor antagonist bosentan prevents and reverses hypoxic pulmonary hypertension in rats. *J Appl Physiol* **79**:2122–2131.
6. **Clozel M, Hess P, Rey M, Iglarz M, Binkert C, Qiu C.** 2006. Bosentan, sildenafil, and their combination in the monocrotaline model of pulmonary hypertension in rats. *Exp Biol Med (Maywood)* **231**: 967–973.
7. **Corno AF, Tozzi P, Genton CY, von Segesser LK.** 2003. Surgically induced unilateral pulmonary hypertension: time-related analysis of a new experimental model. *Eur J Cardiothorac Surg* **23**:513–517.
8. **Das M, Dempsey EC, Reeves JT, Stenmark KR.** 2002. Selective expansion of fibroblast subpopulations from pulmonary artery adventitia in response to hypoxia. *Am J Physiol Lung Cell Mol Physiol* **282**:L976–L986.
9. **De Canniere D, Stefanidis C, Brimioulle S, Naeije R.** 1994. Effects of a chronic aortopulmonary shunt on pulmonary hemodynamics in pigs. *J Appl Physiol* **77**:1591–1596.
10. **Drexler ES, Bischoff JE, Slifka AJ, McCowan CN, Quinn TP, Shandas R, Ivy DD, Stenmark KR.** 2008. Stiffening of the extrapulmonary arteries from rats in chronic hypoxic pulmonary hypertension. *J Res Natl Inst Stand Technol* **113**:239–249.
11. **Ferguson DJ, Berkas EM, Varco RL.** 1953. Circulatory factors contributing to alterations in pulmonary vascular histology. *Surg Forum* **4**:267–270.
12. **Frasch HF, Marshall C, Marshall BE.** 1999. Endothelin 1 is elevated in monocrotaline pulmonary hypertension. *Am J Physiol* **276**:L304–L310.
13. **Galie N, Badesch D, Oudiz R, Simonneau G, McGoon MD, Keogh AM, Frost AE, Zwicke D, Naeije R, Shapiro S, Olschewski H, Rubin LJ.** 2005. Ambrisentan therapy for pulmonary arterial hypertension. *JACC* **46**:529–535.
14. **Galie N, Ghofrani HA, Torbicki A, Barst RJ, Rubin LJ, Badesch D, Fleming T, Parpia T, Burgess G, Branzi A, Grimminger F, Kurzyna M, Simonneau G.** 2005. Sildenafil citrate therapy for pulmonary arterial hypertension. *N Engl J Med* **353**:2148–2157.
15. **Guignabert C, Raffestin B, Benferhat R, Raoul W, Zadigue P, Rideau D, Hamon M, Adnot S, Eddahibi S.** 2005. Serotonin transporter inhibition prevents and reverses monocrotaline pulmonary hypertension in rats. *Circulation* **111**:2812–2819.
16. **Gust R, Schuster DP.** 2001. Vascular remodeling in experimentally induced subacute canine pulmonary hypertension. *Exp Lung Res* **27**:1–12.
17. **Hallioglu O, Dilber E, Celiker A.** 2003. Comparison of acute hemodynamic effects of aerosolized and intravenous iloprost in secondary pulmonary hypertension in children with congenital heart disease. *Am J Cardiol* **92**:1007–1009.
18. **Institute for Laboratory Animal Research.** 1996. Guide for the care and use of laboratory animals. Washington (DC): National Academies Press.
19. **Ivy DD, McMurtry IF, Colvin K, Imamura M, Oka M, Lee DS, Gebb S, Jones PL.** 2005. Development of occlusive neointimal lesions in distal pulmonary arteries of endothelin B receptor-deficient rats: a new model of severe pulmonary arterial hypertension. *Circulation* **111**:2988–2996.
20. **Jungebluth P, Ostertag H, Macchiarini P.** 2008. An experimental animal model of postobstructive pulmonary hypertension. *J Surg Res* **147**:75–78.
21. **Kim H, Yung GL, Marsh JJ, Konopka RG, Pedersen PG, Morris TA, Channick RN.** 2000. Endothelin mediates pulmonary vascular

- remodeling in a canine model of chronic pulmonary hypertension. *Eur Respir J* 15:640–648.
22. Kolettis T, Vlahos AP, Louka M, Hatzistergos KE, Baltogiannis GG, Agelaki MM, Mitsi A, Malamou-Mitsi V. 2007. Characterization of a rat model of pulmonary arterial hypertension. *Hellenic J Cardiol* 48:206–210.
 23. Laudi S, Steudel W, Jonscher K, Schoning W, Schniedewind B, Kaisers U, Christians U, Trump S. 2007. Comparison of lung proteome profiles in 2 rodent models of pulmonary arterial hypertension. *Proteomics* 7:2469–2478.
 24. Maiya S, Hislop AA, Flynn Y, Haworth SG. 2006. Response to bosentan in children with pulmonary hypertension. *Heart* 92:664–670.
 25. Marecki JC, Cool CD, Parr JE, Beckey VE, Luciw PA, Tarantal AF, Carville A, Shannon RP, Cotal-Gomez A, Tuder RM, Voelkel NF, Flores SC. 2006. HIV1 Nef is associated with complex pulmonary vascular lesions in SHIV-nef-infected macaques. *Am J Respir Crit Care Med* 174:437–445.
 26. Mathew R, Zeballos GA, Tun H, Gewitz MH. 1995. Role of nitric oxide and endothelin 1 in monocrotaline-induced pulmonary hypertension. *Cardiovasc Res* 30:739–746.
 27. Medhora M, Bousamra M 2nd, Zhu D, Somberg L, Jacobs ER. 2002. Upregulation of collagens detected by gene array in a model of flow-induced pulmonary vascular remodeling. *Am J Physiol Heart Circ Physiol* 282: H414–H422.
 28. Muller WH, Dammann JF, Head WH. 1953. Changes in the pulmonary vessels produced by experimental pulmonary hypertension. *Surgery* 34:363–375.
 29. Nishimura T, Faul JL, Berry GJ, Kao PN, Pearl RG. 2003. Effect of aortocaval fistula on monocrotaline-induced pulmonary hypertension. *Crit Care Med* 31:1213–1218.
 30. Okada M, Yamashita C, Okada M, Okada K. 1995. Establishment of canine pulmonary hypertension with dehydromonocrotaline: importance of a larger animal model for lung transplantation. *Transplantation* 60:9–13.
 31. Olschewski H, Simonneau G, Galie N, Higenbottam T, Naeije R, Rubin LJ, Nikkho S, Speich R, Hoepfer MM, Behr J, Winkler J, Sitbon O, Popov W, Ghofrani HA, Manes A, Kiely DG, Ewert R, Meyer A, Corris PA, Delcroix M, Gomez-Sanchez M, Siedentop H, Seeger W. 2002. Aerosolized iloprost randomized study group. Inhaled iloprost for severe pulmonary hypertension. *N Engl J Med* 347:322–329.
 32. Parviz M, Bousamra M 2nd, Chammas JH, Birks EK, Presberg KW, Jacobs ER, Nelin LD. 1999. Effects of chronic pulmonary overcirculation on pulmonary vasomotor tone. *Ann Thorac Surg* 67: 522–527.
 33. Perkett EA, Davidson JM, Meyrick B. 1991. Sequence of structural change and elastin peptide release during vascular remodeling in sheep with chronic pulmonary hypertension induced by air embolization. *Am J Pathol* 139:1319–1332.
 34. Rendas A, Reid L. 1979. Aorta-pulmonary shunts in growing pigs. Functional and structural assessment of the changes in the pulmonary circulation. *J Thorac Cardiovasc Surg* 77:109–118.
 35. Rondelet B, Kerbaul F, Motte S, van Beneden R, Rimmelink M, Brimiouille S, McEntee K, Wauthy P, Salmon I, Ketelsegers JM, Naeije R. 2003. Bosentan for the prevention of overcirculation-induced experimental pulmonary arterial hypertension. *Circulation* 107:1329–1335.
 36. Rosenkrantz JG, Carlisle JH, Lynch FP, Vogel JH. 1973. Ligation of a single pulmonary artery in the pig: a model of chronic pulmonary hypertension. *J Surg Res* 15:67–73.
 37. Rosenzweig EB, Barst RJ. 2009. Pulmonary arterial hypertension in children: a medical update. *Indian J Pediatr* 76:77–81.
 38. Rosenzweig EB, Ivy DD, Widlitz A, Doran A, Claussen LR, Yung D, Abman SH, Morganti A, Nguyen N, Barst RJ. 2005. Effects of long-term bosentan in children with pulmonary arterial hypertension. *JACC* 46:697–704.
 39. Rosenzweig EB, Widlitz AC, Barst RJ. 2004. Pulmonary arterial hypertension in children. *Pediatr Pulmonol* 38:2–22.
 40. Rothman A, Mann DM, Behling CA, Konopa RG, Chiles PG, Pedersen CA, Moser KM. 1998. Percutaneous pulmonary endoarterial biopsy in an experimental model of pulmonary hypertension. *Chest* 114:241–250.
 41. Rothman A, Mann D, Behling CA, McGraw M, Seslar S, Shiu P, Zhang L, Kriett J. 2003. Increased expression of endoarterial vascular cell adhesion molecule 1 mRNA in an experimental model of lung transplant rejection: diagnosis by pulmonary arterial biopsy. *Transplantation* 75:960–965.
 42. Rothman A, Mann DM, House MT, Konopka RG, Chiles PG, Pedersen CA, Wolf P, Moser KM. 1996. Transvenous procurement of pulmonary artery smooth muscle and endothelial cells using a novel endoarterial biopsy catheter in a canine model. *J Am Coll Cardiol* 27:218–224.
 43. Sato H, Hall CM, Griffith GW, Johnson KF, McGillicuddy JW, Bartlett RH, Cook KE. 2008. Large animal model of chronic pulmonary hypertension. *ASAIO Journal* 54:396–400.
 44. Schermuly RT, Kreisselmeier KP, Ghofrani HA, Yilmaz H, Butrous G, Ermer L, Ermer M, Weissmann N, Rose F, Guenther A, Walmrath D, Seeger W, Grimminger F. 2004. Chronic sildenafil treatment inhibits monocrotaline-induced pulmonary hypertension in rats. *Am J Resp Crit Care Med* 169:39–45.
 45. Shelub I, van Grondelle A, McCullogh R, Hofmeister S, Reeves JT. 1984. A model of embolic chronic pulmonary hypertension in the dog. *J Appl Physiol* 56:810–815.
 46. Simonneau G, Barst RJ, Galie N, Naeije R, Rich S, Bourge RC, Keogh A, Oudiz R, Frost A, Blackburn SD, Crow JW, Rubin LJ; Treprostinil Study Group. 2002. Continuous subcutaneous infusion of treprostinil, a prostacyclin analogue, in patients with pulmonary arterial hypertension: a double-blind, randomized, placebo-controlled trial. *Am J Respir Crit Care Med* 165:800–804.
 47. Song Y, Jones JE, Beppu H, Keaney JF Jr, Loscalzo J, Zhang YY. 2005. Increased susceptibility to pulmonary hypertension in heterozygous BMPR2-mutant mice. *Circulation* 112:553–562.
 48. Stenmark KR, Fagan KA, Frid MG. 2006. Hypoxia-induced pulmonary vascular remodeling: cellular and molecular mechanisms. *Circ Res* 99:675–691.
 49. Stenmark KR, Fasules J, Hyde DM, Voelkel NF, Henson J, Tucker A, Wilson H, Reeves JT. 1987. Severe pulmonary hypertension and arterial adventitia changes in newborn calves at 4300 m. *J Appl Physiol* 62:821–830.
 50. Sugiura T, Suzuki S, Hussein MH, Kato T, Togari H. 2003. Usefulness of a new Doppler index for assessing both ventricular functions and pulmonary circulation in newborn piglets with hypoxic pulmonary hypertension. *Pediatr Res* 53:927–932.
 51. Van Loon RL, Hoendermis ES, Duffels MG, Vonk-Noordegraaf A, Mulder BJ, Hillege HL, Berger RM. 2007. Long-term effect of bosentan in adults versus children with pulmonary arterial hypertension associated with systemic-to-pulmonary shunt: does the beneficial effect persist? *Am Heart J* 154:776–782.
 52. West J, Fagan K, Steudel W, Fouty B, Lane K, Harral J, Hoedt-Miller M, Tada Y, Ozimek J, Tuder R, Rodman DM. 2004. Pulmonary hypertension in transgenic mice expressing a dominant-negative BMPRII gene in smooth muscle. *Circ Res* 94:1109–1114.
 53. White RJ, Meoli DF, Swarhout RF, Kallop DY, Galaria II, Harvey JL, Miller CM, Blaxall BC, Hall CM, Pierce RA, Cool CD, Taubman MB. 2007. Plexiform-like lesions and increased tissue factor expression in a rat model of severe pulmonary hypertension. *Am J Physiol Lung Cell Mol Physiol*. 293:L583–L590.